



# Structural and electrochemical studies of bromide derived ionic liquid-based gel polymer electrolyte for energy storage application

Ashish Gupta<sup>a</sup>, Amrita Jain<sup>b</sup>, S.K. Tripathi<sup>c,\*</sup>

<sup>a</sup> Government Tulsi Degree College, Anuppur, Madhya Pradesh 484224, India

<sup>b</sup> Institute of Fundamental Technological Research, Polish Academy of Sciences, Adolfa Pawińskiego 5b, 02-106 Warsaw, Poland

<sup>c</sup> Department of Physics, School of Physical Sciences, Mahatma Gandhi Central University, Bihar 845401, India

## ARTICLE INFO

### Keywords:

Gel polymer electrolytes  
Ionic liquid  
Solution cast technique  
Supercapacitors

## ABSTRACT

In the present studies, poly (vinylidene fluoride-co-hexafluoropropylene) (PVDF-HFP), ionic liquid {1-Ethyl-3-methylimidazolium bromide} (EMIM)(Br), and magnesium perchlorate  $Mg(ClO_4)_2$  as salt were used to synthesize free standing electrolyte films by using solution cast technique. The prepared electrolyte films were investigated by using various structural and electrochemical techniques like scanning electron microscopy (SEM), X-ray diffraction analysis (XRD), Fourier transform infrared spectroscopy (FTIR) and differential scanning calorimetry (DSC) as well as ionic and temperature dependence studies. It has been observed that addition of ionic liquid significantly increases the properties like ionic conductivity, thermal stability, transparency etc. The maximum room temperature ionic conductivity for the optimized system was found to be of the order of  $2.05 \times 10^{-2} S cm^{-1}$  which is suitable for device fabrication point of view. The optimized electrolyte films are suitable for supercapacitor application.

## 1. Introduction

The performance parameters like overall capacity, energy, power and current density, cyclability, operating voltage, time stability and most importantly safety of any electrochemical device depends on the electrolyte materials [1–3]. To satisfy the above criteria, solid state electrolytes are one of the solutions, as it overcomes all the restrictions of its liquid like nature like leakage, gas formation due to solvent decomposition, volatile and thermal instability [4]. For the reason, research communities are attracting towards the development of dry electrolytes by introducing different conducting materials in polymer matrix or by polymerization of such materials [4–5]. In this situation, ion conducting polymer electrolytes has received worldwide attention due to their intrinsic properties like transparency, ability to cast into thin film, flexibility, dimensional stability, high ionic conductivity and wide electrochemical window [6–7]. Development of such kind of materials broadened the array of applications like lithium ion batteries, supercapacitors, solar cells, fuel cells, capacitors, solid state batteries etc. with high temperature stability and improved safety [8].

Gel polymer electrolytes (GPEs) consists of polymer matrices, conducting inorganic/organic salt and plasticizer, which possess many advantages like shape flexibility, interface stability and manufacturing integrity [9]. Because of their unique hybrid structure, gel polymer

electrolytes simultaneously possess cohesive properties of solids and diffusive properties of liquids which is responsible for their unique properties suitable for electrochemical applications [10–12].

Many research groups have reported the GPEs which consists of plasticizers such as propylene carbonate (PC), ethylene carbonate (EC), dimethyl carbonate (DMC), diethyl carbonate (DEC) and dimethyl formamide (DMF) [12–14]. These plasticizers help in reducing the degree of crystallinity of the synthesized polymers electrolytes, enhance the flexibility along with amorphicity of the polymer chain and certainly improves the ionic conductivity of the system [13]. For instance, in the presence of EC and DEC in certain fixed ratio, the ionic conductivity of the gel polymer electrolyte using poly (vinylidene fluoride-co-hexafluoropropylene) (PVDF-HFP) as polymer and lithium perchlorate ( $LiClO_4$ ) salt was found to be of the order of  $\sim 1.06 \times 10^{-3} S cm^{-1}$ . But it has been reported that these organic plasticizers lack safety owing to their volatile and flammable nature [15–16]. Arbizzani et al. [17] has performed flammability studies on traditional organic mixture EC-DMC- $LiPF_6$ . Hence in view of safety, it was reported that the mixture with sufficiently high content of ionic liquid *N*-butyl-*N*-methylpyrrolidinium bis(tri-fluoromethane-sulfonyl)imide was less volatile and flammable [17].

Ionic liquids (ILs) consist of bulky and asymmetric organic cations and inorganic anions with properties like wide electrochemical

\* Corresponding author.

E-mail addresses: [ajain@ippt.pan.pl](mailto:ajain@ippt.pan.pl) (A. Jain), [sktripathi@mgcub.ac.in](mailto:sktripathi@mgcub.ac.in) (S.K. Tripathi).

window, non-flammability, negligible vapour pressure, excellent thermal and chemical stability with very high ionic conductivity which makes them suitable replacements for plasticizers and salts in polymer electrolytes [17–18]. Though despite the fact that, polymers are the best candidates to immobilize ILs, only few polymers and fewer ILs are used till now. But the flexibility of IL and polymer chemistry certainly allows research community to develop an infinite number of ionogel [19]. Thus, the vast field of ionogel membranes are yet to explore, since the different combinations of IL and host polymers opens significant options for electrochemical devices.

PVdF-HFP is one of the promising candidates of polymeric materials with high dielectric constant  $\sim 8.4$ , and has a good potential to act as a host polymer to produce electrolyte films. PVdF-HFP contains predominantly crystalline PVdF phase and amorphous VdF phase which facilitates necessary mechanical strength and simultaneously good ion transport matrix. PVdF-HFP with ILs have been reported with ionic conductivity close to  $10 \text{ mS cm}^{-1}$ , good thermal stability up to  $310^\circ\text{C}$  [20], wide electrochemical window up to 4–5 V [21] and free standing mechanically stable films [22]. In the present studies, magnesium ion-based salt has been chosen owing to the fact that Mg is environment friendly, inexpensive and safe as compared to lithium, further it has difficulty in dendrite formation and low reduction potential ( $-2.37 \text{ V}$  vs. SHE) which is a big advantage [23–24].

In the present studies, ionic liquid based gel polymer electrolyte films PVdF-HFP/{1-Ethyl-3-methylimidazolium bromide} (EMIM)(Br)/PC/magnesium perchlorate  $\text{Mg}(\text{ClO}_4)_2$  were prepared and optimized, its detailed investigations were carried out by using SEM, XRD, FTIR and DSC measurements and finally ionic conductivity and temperature dependent conductivities were also studied.

## 2. Materials and methods

### 2.1. Synthesis of gel polymer electrolyte films

The ionic liquid {1-Ethyl-3-methylimidazolium bromide} (EMIM)(Br), host polymer poly(vinylidene fluoride-co-hexafluoropropylene) [PVdF(HFP)] (Average MW  $\sim 400,000$ ), and the salt magnesium perchlorate  $\text{Mg}(\text{ClO}_4)_2$  were obtained from Sigma Aldrich, propylene carbonate (PC) as plasticizer from Loba Chemie and acetonitrile (ACN) as an intermediate solvent from Merck, Germany was used to prepare ionic liquid-based gel polymer electrolyte films. All the chemicals were used without further purifications. The ionic liquid-based gel polymer electrolyte films [PVdF(HFP) - (EMIM)(Br) - PC- $\text{Mg}(\text{ClO}_4)_2$ ] were prepared by using "Solution Cast" method. Fig. 1 shows the block diagram for the synthesis of electrolyte films.

In the process, initially, the liquid electrolyte was prepared by

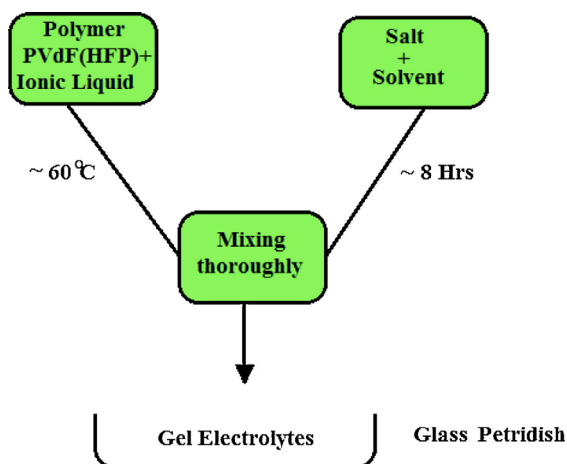


Fig. 1. Flowchart of the synthesis of polymer gel electrolyte.

dissolving different concentrations of magnesium salt,  $\text{Mg}(\text{ClO}_4)_2$  in propylene carbonate (PC). The different weight percent of the polymer, PVdF(HFP) and (EMIM)(Br) were dissolved separately in common solvent acetonitrile (ACN). The optimized composition of liquid electrolyte was then mixed with the optimized solution of PVdF(HFP)- (EMIM)(Br)-ACN in different weight ratios and stirred thoroughly for  $\sim 8 \text{ h}$ . The final optimized composition was found to be [(PVdF(HFP) - (EMIM)(Br))(3:7)] (30 wt%) - [PC -  $\text{Mg}(\text{ClO}_4)_2$  (0.3M)] (70wt%). The obtained viscous mixture was then cast over glass petri-dishes and ACN was allowed to evaporate slowly, thereafter, free-standing polymer gel electrolyte films ( $400\text{--}500 \mu\text{m}$ ) were obtained.

### 2.2. Instrumental details

X-ray diffraction (XRD) patterns of the synthesized films are recorded using Bruker D8 Advance diffractometer with  $\text{Cu-K}\alpha$  radiation over the Bragg angle ( $2\theta$ ) range of  $10\text{--}60^\circ$ . The scan rate was fixed at  $5^\circ \text{ min}^{-1}$ . The surface morphology of the polymer gel electrolyte was studied with the help of scanning electron microscope (SEM) using JEOL JXA - 8100 EPMA. The samples were coated by gold in order to make its surface conducting for taking measurements under low vacuum. Fourier transform infrared (FTIR) spectra of the polymeric systems were recorded using Bruker vertex 70 spectrophotometer. The thermal analysis of the polymer gel systems was carried out using differential scanning calorimetry (DSC) from  $-70$  to  $175^\circ\text{C}$  at a heating rate of  $10^\circ\text{C min}^{-1}$  in presence of nitrogen atmosphere with the help of Mettler Toledo DSC 822E. The electrical conductivity of polymer gel electrolytes was measured by means of an ac impedance spectroscopic techniques with the help of LCR Hi-Tester (HIOKI-3522-50, Japan) over the frequency range of  $100 \text{ kHz}$  to  $1 \text{ Hz}$  with a signal level of  $10 \text{ mV}$ . The samples were cut into a proper size and sandwiched between two stainless steel electrodes for taking the conductivity measurements. The ionic transport number and electrochemical stability of the polymer gel electrolytes were carried out by CHI 608C, CH Instruments, USA.

## 3. Results and discussion

The ionic conductivity of the optimized system is found to be ( $\sigma = 2.05 \times 10^{-2} \text{ S cm}^{-1}$ ). In the process of synthesizing polymer gel electrolytes, polymer/ionic liquid blend has been synthesized and optimized separately after optimization of liquid electrolytes. Fig. 2 shows the variation of electrical conductivity of polymer/ionic liquid blend PVdF(HFP)-EMIM(Br), as a function of ionic liquid EMIM(Br) concentration. From Fig. 2 it can be seen that on the addition of different

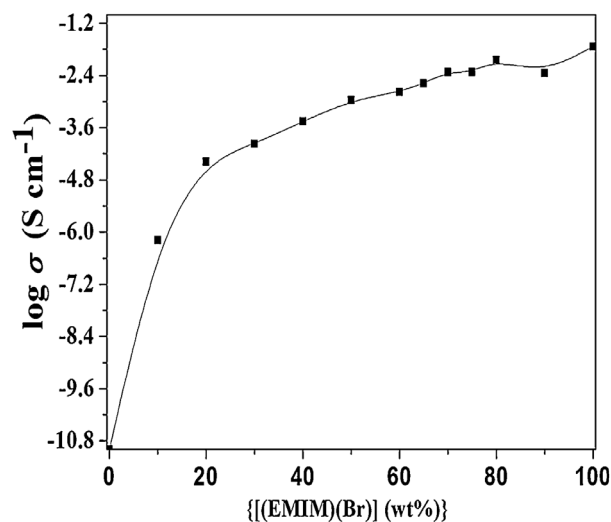


Fig. 2. Room temperature electrical conductivity of polymer/ionic liquid blend as a function of ionic liquid concentration.

weight percent of ionic liquid EMIM(Br) in host polymer PVdF(HFP), the conductivity of blend system suddenly increases up to four orders ( $10^{-10} \text{ S cm}^{-1}$  to  $10^{-6} \text{ S cm}^{-1}$ ) by the addition of small concentration of ionic liquid (~10 wt %). On further addition of ionic liquid concentration beyond 10 wt %, it has been observed that the conductivity gradually increases up to 70 wt % ( $\sigma = 4.82 \times 10^{-3} \text{ S cm}^{-1}$ ) and thereafter remains constant.

The enhancement in electrical conductivity of the polymer/ionic liquid blend can be explained on the basis of plasticization effect which produces flexibility in polymer matrix and generation of free ions, namely;  $(\text{EMIM})^+$  and  $(\text{Br})^-$  in the system leads to the enhancement in conductivity. Further it was also observed that film was not stable beyond 70 wt % of ionic liquid concentration. Hence finally polymer/ionic liquid blend having composition of PVdF(HFP)-EMIM(Br) (3:7) has been chosen for the synthesis of polymer gel electrolytes.

Finally, the polymer gel electrolyte comprising of PVdF(HFP) - EMIM(Br) - PC-Mg(ClO<sub>4</sub>)<sub>2</sub> was synthesized and optimized by immobilizing different weight percentage of the optimum concentration of polymer/ionic liquid blend, PVdF(HFP)-EMIM(Br) (3:7) in the solution of optimized liquid electrolyte PC-Mg(ClO<sub>4</sub>)<sub>2</sub> (0.3 M) system as shown in Fig. 3.

From Fig. 3 it can be seen that the initial conductivity of liquid electrolyte without blend is  $3.63 \times 10^{-3} \text{ S cm}^{-1}$ . On the addition of different weight percent of optimum blend concentration, PVdF(HFP)-EMIM(Br) (3:7) in the optimized liquid electrolyte PC-Mg(ClO<sub>4</sub>)<sub>2</sub> (0.3 M) solution, the electrical conductivity of polymer gel electrolytes initially increases and shows a maxima at 30 wt % ( $\sigma = 2.05 \times 10^{-2} \text{ S cm}^{-1}$ ) and thereafter it starts decreasing on its further addition. It has been observed that polymer gel electrolyte film is mechanically unstable below 30 wt % of polymer/ionic liquid blend concentration. The stable film is obtained only after 30 wt % of the blend concentration. Such types of increase in conductivity behaviour of the polymer gel electrolyte on addition of polymeric concentration has been reported earlier by some workers [25–26] in a different polymeric system. Finally, ionic liquid based polymer gel electrolytes having optimized composition of [PVdF(HFP) (30wt%) - EMIM(Br) (70wt%)] (30 wt%) - [PC-Mg(ClO<sub>4</sub>)<sub>2</sub> (0.3M)] (70 wt%) has been chosen for its further studies.

The variation of ionic conductivity as a function of temperature for the optimized composition of polymer gel electrolyte are shown in Fig. 4.

From the plot it can be seen that the electrical conductivity shows

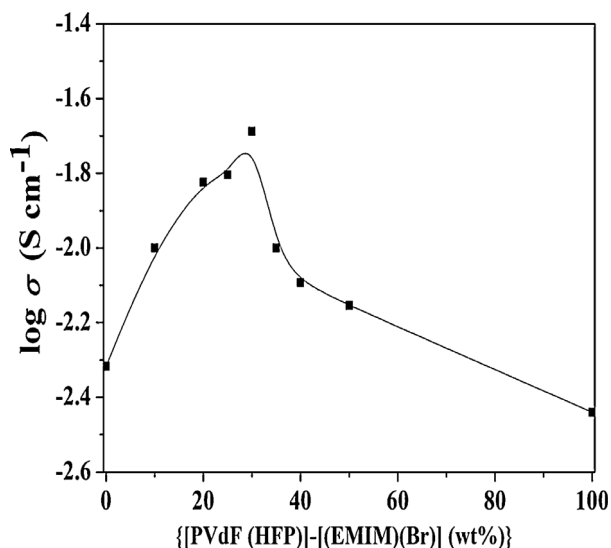


Fig. 3. Variation of electrical conductivity of polymer gel electrolyte as a function of polymer/ionic liquid blend concentration.

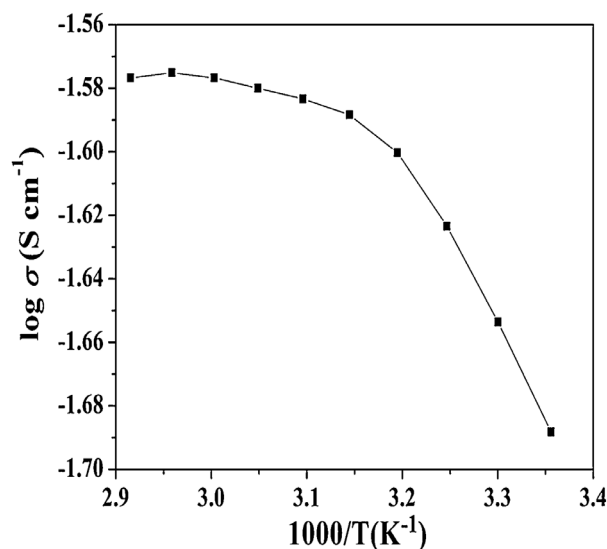


Fig. 4. Variation of electrical conductivity of optimized polymer gel electrolytes as a function of temperature.

non-linear pattern with respect to temperature, which suggests that the segmental motion of polymer is mainly responsible for ion transport in polymer gel electrolyte systems. This result may be well explained on the basis of Vogel-Tamman-Fulcher (VTF) equation as mentioned below:

$$\sigma = AT^{-1/2} \exp\left(\frac{-B}{T - T_0}\right)$$

where 'A' represents pre-exponential factor and is proportional to the number of charge carriers, 'B' is a fitting constant and is related to its pseudo-activation energy and 'T<sub>0</sub>' is the equilibrium temperature of the system corresponding to zero entropy configuration.

It has been observed that as the temperature of polymer gel electrolyte increases its electrical conductivity also increases. The increase in temperature increases the vibrational energy of a polymeric chain, which thereby pushes its neighbouring atoms and creates some free space around its own volume in which vibrational motion can easily occur. This segmental motion of polymeric chain permits the ion to hop from one site to another and provides them a pathway to move, which leads to the enhancement in conductivity of the polymer gel electrolyte system. Hence the combined effect of increased free volume, segmental motion of polymeric chain and ion mobility of charge carriers are mainly responsible for enhancement in the electrical conductivity of the system. Different parameters associated with the VTF model of polymer gel electrolyte system such as A, B, T<sub>0</sub>, has been evaluated by non-linear least square fitting of the data and are listed in Table 1.

Liquid-like transport of ions which are confined in liquid electrolyte and trapped in a polymer matrix and the polymer-swelled gel phase with liquid electrolyte are two main factors which plays a key role in better ion transport in gel polymer electrolytes [27]. The surface morphologies of pure polymer, optimized composition of polymer/ionic liquid blend and polymer gel electrolytes are shown in Fig. 5 (a-c) respectively. From Fig. 5(a) it can be seen that the pure PVdF(HFP) film

Table 1

Parameter (A, B and T<sub>0</sub>) for ionic liquid based polymer gel polymer electrolyte obtained by non-linear least square fitting of conductivity data to VTF equation.

Sample	Parameters		
	A(S cm <sup>-1</sup> ) K <sup>-1/2</sup>	B(eV)	T <sub>0</sub> (K)
Optimized polymer film	0.0481	0.02	292

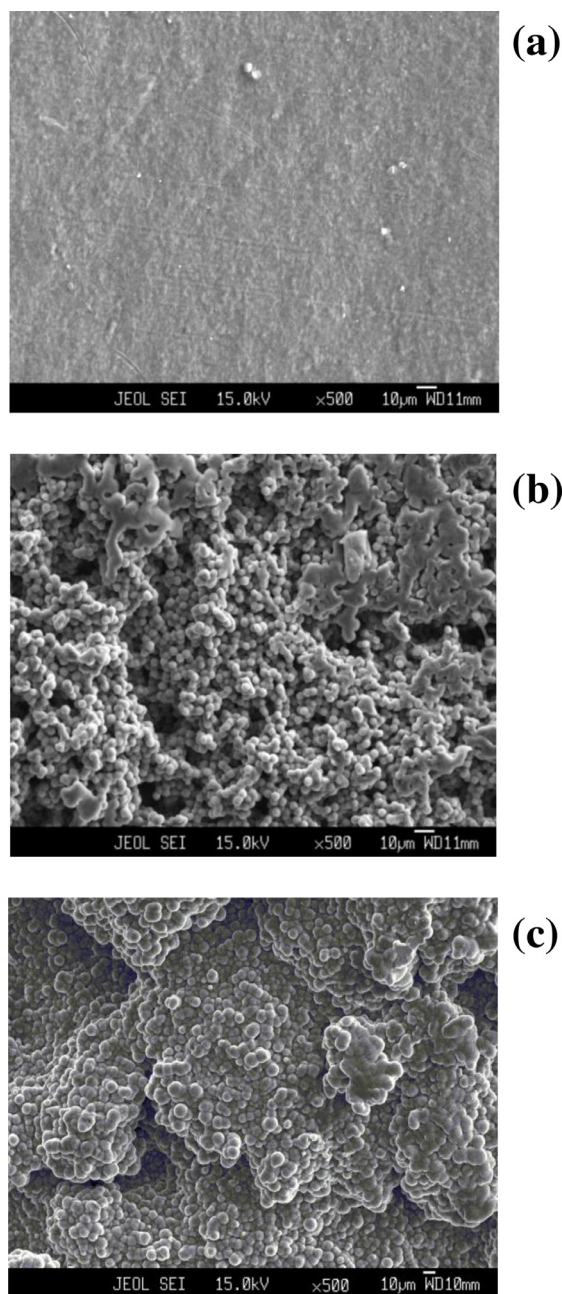


Fig. 5. SEM image of (a) pure PVdF(HFP) film (b) [PVdF(HFP)-EMIM(Br)] (3:7) polymer/ionic liquid blend (c) [{PVdF(HFP)-EMIM(Br)}(3:7)] (30 wt%) - [PC-Mg(ClO<sub>4</sub>)<sub>2</sub>](0.3M)] (70 wt%) polymer gel electrolytes.

shows the presence of uniformly distributed and interconnected pores in its matrix. On addition of ionic liquid and liquid electrolytes in the host polymer, its morphology gets changed. It can be seen from Fig. 5(b) that polymer/ionic liquid blend exhibits a small pore having almost uniform size.

On addition of liquid electrolytes in the polymer/ionic liquid blend, it is observed that polymer gel electrolytes have slightly larger and uniformly distributed pore size as can be seen from Fig. 5(c). This uniformly distributed pore sizes are mainly responsible for the retention of ionic liquid and liquid electrolyte solution in it which further leads to the enhancement in the electrical conductivity by providing better connectivity through its branched network. XRD studies has also been carried out in order to confirm the changes occurring in the semi-crystalline characteristics of host polymer PVdF(HFP) on the addition of ionic liquid and liquid electrolytes. Fig. 6 (a-e) shows the XRD pattern

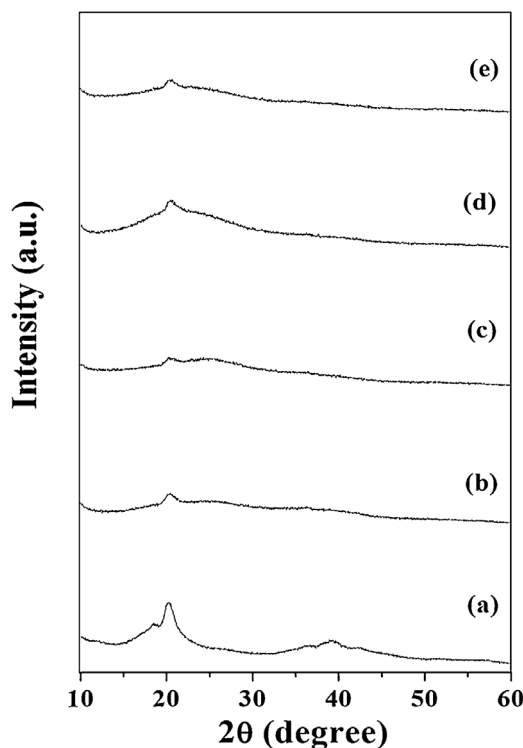


Fig. 6. XRD pattern of (a) Pure PVdF(HFP) film (b) [PVdF(HFP)-EMIM(Br)] (4:6) (c) [PVdF(HFP)-EMIM(Br)] (3:7) polymer/ionic liquid blends (d) [{PVdF(HFP)-EMIM(Br)}(3:7)] (30wt%)-[PC-Mg(ClO<sub>4</sub>)<sub>2</sub>] (70wt%) and (e) [{PVdF(HFP)-EMIM(Br)}(3:7)] (20wt%)-[PC-Mg(ClO<sub>4</sub>)<sub>2</sub>(0.3M)](80wt%) polymer gel electrolytes.

of pure polymer PVdF(HFP), polymer-ionic liquid blend PVdF(HFP) - EMIM(Br) and polymer gel electrolytes PVdF(HFP) - EMIM (Br) - PC-Mg(ClO<sub>4</sub>)<sub>2</sub> films.

Fig. 6(a) shows the semi-crystalline nature of host polymer PVdF(HFP) in which the predominant peaks appear at  $2\theta = 20^\circ$  and  $38^\circ$  corresponds to (020) and (021) of its crystalline peaks. On addition of ionic liquid EMIM(Br) in host polymer PVdF(HFP), peak appearing at  $38^\circ$  gets almost disappeared and intensity of the peak corresponding to  $20^\circ$  gets reduced, as can be seen from Fig. 6(b-c). On further addition of liquid electrolytes PC-Mg(ClO<sub>4</sub>)<sub>2</sub> in polymer-ionic liquid blend, intensity of the peak at  $2\theta = 20^\circ$  further reduces in the polymer gel electrolytes as shown in Fig. 6(d-e). The disappearance of PVdF(HFP) peak at  $2\theta = 38^\circ$  and reduction in the intensity observed at  $20^\circ$  suggests that polymer/ionic liquid blend and polymer gel electrolytes are predominantly amorphous in nature which further supports the electrical conductivity of the polymeric system. It also confirms the complete complexation of ionic liquid and liquid electrolytes with the host polymer PVdF(HFP) at microscopic level. Based on this broad peak, the Debye-Scherrer equation given below is employed for the analysis of crystalline size:

$$d = \frac{K\lambda}{\beta \cos\theta}$$

where K is the constant,  $\lambda$  is the X-ray wavelength at  $1.54 \text{ \AA}$  for CuK $\alpha$  radiation,  $\beta$  is the particle broadening and  $\theta$  is the position at which the broadening occurred. According to this equation, particle size (d) and peak length ( $\beta$ ) are inversely proportional to each other. In other words, broader is the peak, smaller is the crystalline size. The various parameters such as crystallite size/Scherrer length (l), d-spacing, relative peak intensity of pure salt, polymers, polymer/ionic liquid blend and polymer gel electrolytes has been calculated from XRD plot and using above equation are tabulated in Table 2.

Fourier transform infrared (FTIR) spectroscopy is one of the most

**Table 2**  
X-ray diffraction (XRD) data of ionic liquid-based polymer gel electrolytes.

Sample	2 $\theta$ (deg)	$\theta$	d(Å)	l(Å)	Intensity
Pure PVdF(HFP)	20.4	10.2	4.52	0.22	100
[PVdF(HFP)-EMIM(Br)](3:7)	20.26	10.13	4.4	0.18	100
[PVdF(HFP)-EMIM(Br)](4:6)	20.46	10.23	4.2	0.18	100
[PVdF(HFP)-EMIM(Br)(3:7)] (30wt%) -[(PC-Mg(ClO <sub>4</sub> ) <sub>2</sub> )(0.3M)] (70wt%)	20.46	10.23	4.5	0.17	100
[PVdF(HFP)-BDiMIM(Cl)(3:7)] (20wt%) -[(PC-Mg(ClO <sub>4</sub> ) <sub>2</sub> )(0.3M)] (80wt%)	20.53	10.26	4.5	0.17	100

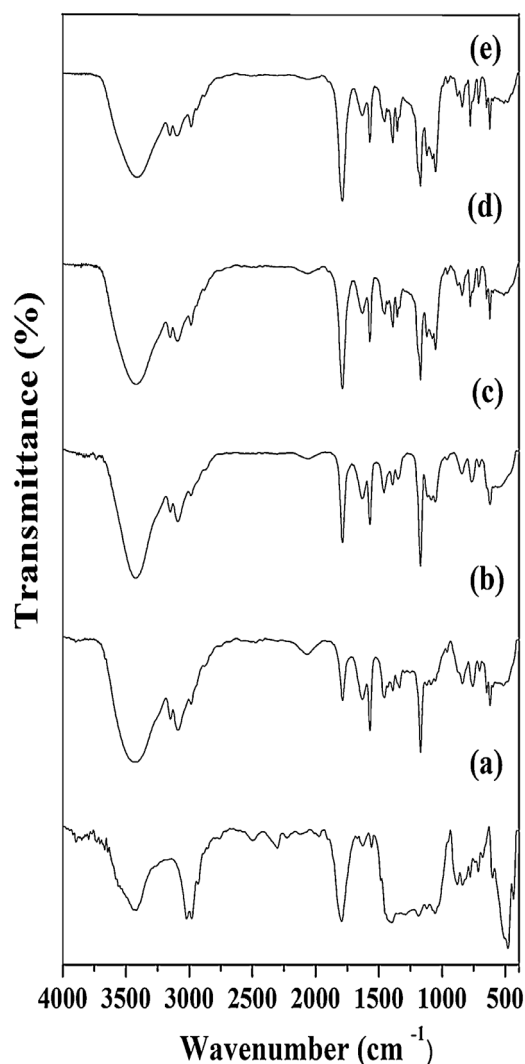


**Fig. 7.** FTIR Spectra of (a) pure PVdF(HFP), (b) [PVdF(HFP)-EMIM(Br)](3:7) blend, different ratios of polymer gel electrolytes [PVdF(HFP)-EMIM(Br)](3:7)] - [(PC-Mg(ClO<sub>4</sub>)<sub>2</sub>)(0.3M))], (c) (2:8), (d) (3:7) and (e) (4:6) film.

important techniques for the identification of complex formation and interactions amongst the different constituents of the polymeric systems. Fig. 7 shows the FTIR spectra of pure polymer PVdF(HFP), polymer-ionic liquid blend PVdF(HFP)-EMIM(Br) and polymer gel electrolytes PVdF(HFP)-EMIM(Br)-PC-Mg(ClO<sub>4</sub>)<sub>2</sub> within a frequency range of 400–4000 cm<sup>-1</sup>. Fig. 7(a) shows the FTIR spectra of pure polymer PVdF(HFP). The vibrational band observed at 3030 and 2986 cm<sup>-1</sup> corresponds to the symmetric and asymmetric stretching vibrations of CH<sub>2</sub> groups respectively [28]. The strong absorbance at 1793 cm<sup>-1</sup> represents the presence of -CF=CF<sub>2</sub> groups [29]. The peak

observed at wave number 1185 and 1395 cm<sup>-1</sup> is meant for the symmetric and deformation vibrations of -CF<sub>2</sub> group. The vibrational peaks observed at wave number 606, 772, 837 and 880 cm<sup>-1</sup> has been assigned to CF<sub>3</sub> group, CH<sub>2</sub> wagging vibration, CH<sub>2</sub> rocking and out of plane C-H bending of the vinylidene groups respectively [30]. On incorporation of ionic liquid EMIM(Br) in the host polymer PVdF(HFP), it has been observed that some new peaks at wave number 3149, 3088, 1628 and 1570 cm<sup>-1</sup> appears in the polymer-ionic liquid blend system as can be depicted from Fig. 7(b) and (c). The vibration peak appears at wave number 3149 and 3088 is assigned to the asymmetric and symmetric C-H stretching vibrations of aromatic ring present in the ionic liquid EMIM(Br) [31–32]. The new peaks appeared at wave number 1628 cm<sup>-1</sup> is due C=C symmetric stretching and to that of 1570 cm<sup>-1</sup> is due to the stretching of (N)CH<sub>2</sub> bonds of imidazolium ring [33]. Fig. 7 (d) and (e) shows that the spectra of ionic liquid-based polymer gel electrolytes (after the incorporation of liquid electrolytes in polymer/ionic liquid blend) have some additional peaks at wave number 1424, 1052, 922 and 622 cm<sup>-1</sup> respectively. The wave number of 1424, 1052 and 922 cm<sup>-1</sup> corresponds to the vibration of CH<sub>2</sub> bending, C=O stretching and ring breathing mode of the liquid electrolytes (PC-Mg(ClO<sub>4</sub>)<sub>2</sub>) [34].

The vibration peaks at 622 cm<sup>-1</sup> is attributed to the free anions (ClO<sub>4</sub>)<sup>-</sup> in the polymer gel electrolytes [28, 35]. The shifting of peak position towards lower and higher frequency regions in the polymer/ionic liquid blend and polymer gel electrolytes system suggests that the strong interactions of ionic liquid and liquid electrolytes has taken place with the host polymer at microscopic level. Table 3 shows the comparison of band spectra of polymer, polymer/ionic liquid blend and polymer gel electrolytes respectively.

Fig. 8 shows the DSC curves of pure polymer PVdF(HFP), polymer-ionic liquid blend PVdF(HFP)-EMIM(Br) and polymer gel electrolytes PVdF(HFP)-EMIM(Br)-PC-Mg(ClO<sub>4</sub>)<sub>2</sub> respectively. From Fig. 8 (a) it can be seen that the endothermic peak for pure PVdF(HFP) has been observed at ~142°C.

By the addition of ionic liquid EMIM(Br) in host polymer PVdF(HFP), the melting temperature of host polymer gets reduced to ~122°C and in addition to that one another asymmetric hump peak at ~79°C has been observed indicating the presence of additional phase due to the possible interaction of polymer and ionic liquid, as can be seen from Fig. 8 (b). Such types of separate phase are also observed in the case of polymer gel electrolyte film, where the ionic liquid and liquid electrolyte solution gets entrapped in the polymer matrix. It is further observed that the polymer gel electrolytes remain stable in the same gel phase over a wider temperature range of ~-70°C to 108°C, indicating the proper interaction of EMIM(Br), PC-Mg(ClO<sub>4</sub>)<sub>2</sub> with polar PVdF(HFP) at microscopic level.

The calculated values of T<sub>c</sub>, X<sub>c</sub>, ΔH<sub>m</sub> and the crystalline melting temperature (T<sub>m</sub>) for polymer gel electrolytes are presented in Table 4.

The electrolyte has been tested for supercapacitor application with bagasse-based biomass derived electrodes and bromide derived ionic liquid-based electrolyte and the detail results has been published somewhere else [36]. In the studies, the fabricated cell shows the overall specific capacitance of 372 mF cm<sup>-2</sup> which is equivalent to single electrode specific capacitance of 248 F g<sup>-1</sup> with energy and power density of 16.3 Wh kg<sup>-1</sup> and 1.66 kW kg<sup>-1</sup> respectively.

#### 4. Conclusions

Ionic liquid based polymer gel electrolytes film using magnesium salt [(PVdF(HFP)-EMIM(Br))(3:7)] (30 wt%) - [(PC-Mg(ClO<sub>4</sub>)<sub>2</sub>)(0.3 M)] (70 wt%) has been synthesized by standard "solution cast" techniques and the optimized composition offers the ionic conductivity of the order of ~ 2.05 × 10<sup>-2</sup> S cm<sup>-1</sup> at room temperature. XRD and FTIR studies show the proper interaction and complex formation between polymer, ionic liquid and liquid electrolytes. It confirms the increase in amorphicity of the polymeric system, which leads to the enhancement

**Table 3**Assignment of important FTIR bands of pure PVdF(HFP), polymer/ionic liquid blend PVdF(HFP)-EMIM(Br) and polymer gel electrolytes PVdF(HFP)-EMIM(Br)-PC-Mg(ClO<sub>4</sub>)<sub>2</sub> (0.3M).

Band assignments	Pure PVdF (HFP)	[PVdF(HFP)-EMIM(Br)](3:7)	[PVdF(HFP) - EMIM (Br)(3:7)] (20wt%)-[PC-Mg(ClO <sub>4</sub> ) <sub>2</sub> ](0.3 M)] (80wt%)	[PVdF(HFP)- EMIM (Br)(3:7)] (30wt%)-[PC-Mg (ClO <sub>4</sub> ) <sub>2</sub> ](0.3 M)] (70wt%)	[PVdF(HFP)-EMIM(Br) (3:7)] (40wt %)-[PC-Mg (ClO <sub>4</sub> ) <sub>2</sub> ](0.3 M)] (60wt %)
C-H Asym. Stretching of aromatic ring	-	3149	3150	3150	3152
C-H sym. Stretching of aromatic ring	-	3088	3089	3093	3095
Asym. Stretching CH <sub>2</sub>	3020	-	-	-	-
Sym. Stretching CH <sub>2</sub>	2986	2984	2974	2985	2984
-CF=CF <sub>2</sub> stretching vibration	1793	1786	1787	1787	1788
C=C symmetric stretching	-	1628	1629	1629	1629
(N) CH <sub>2</sub>	-	1570	1570	1572	1572
CH <sub>2</sub> bending (PC)	-	-	1424	1424	1426
CF <sub>2</sub> symmetric stretching	1185	1169	1170	1170	1170
C=O stretching (PC)	-	-	1052	1052	1051
Ring stretching mode (PC)	-	-	-	922	922
C-H out of plane bending	880	-	-	880	880
CH <sub>2</sub> rocking	837	839	843	841	840
CH <sub>2</sub> wagging vib.	772	756	766	777	777
(ClO <sub>4</sub> ) <sup>-</sup> ion pairing	-	-	622	621	622

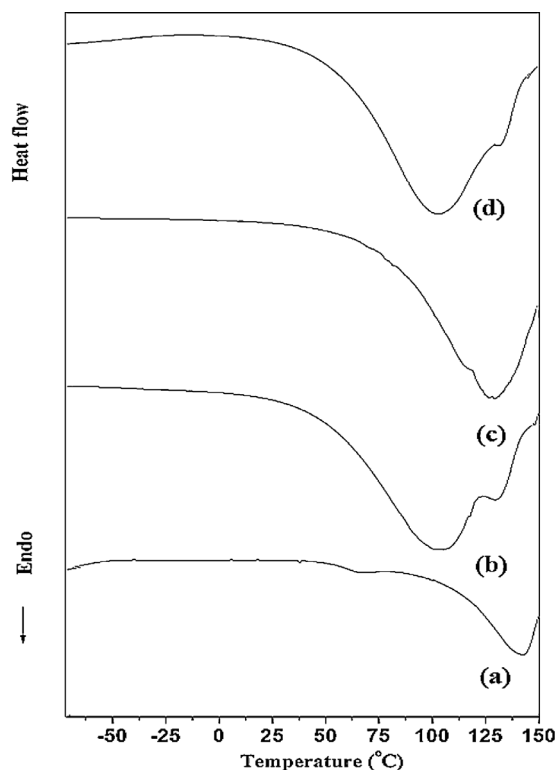


**Fig. 8.** DSC profile of (a) pure PVdF(HFP) film, (b) polymer/ionic liquid blend film [PVdF(HFP)-EMIM(Br)] (4:6) (c) [PVdF(HFP)-EMIM(Br)] (3:7) and (d) polymer gel electrolytes film [PVdF(HFP)-EMIM(Br) (3:7)](30wt%)-[PC-Mg(ClO<sub>4</sub>)<sub>2</sub> (0.3M)] (70wt%).

in electrical conductivity. Surface morphology of the polymer, polymer/ionic liquid blend and ionic liquid-based polymer gel electrolytes system are observed by SEM studies. It shows the porous nature of gel system and having a good liquid electrolytes retention capability that favours the enhancement in electrical conductivity through its polymeric network. DSC studies shows the excellent thermal stability having single-phase behaviour within a temperature range of -70°C to 108°C. The temperature dependence pattern of electrical conductivity shows the VTF behaviour of the polymer gel electrolytes and its activation energy are calculated by the non-linear least square curve fitting

**Table 4**

Thermal properties of ionic liquid-based polymer gel electrolytes.

Sample	T <sub>c</sub> (°C)	T <sub>m</sub> (°C)	ΔH <sub>m</sub> (J g <sup>-1</sup> )	% X <sub>c</sub>
Pure PVdF(HFP)	110	142.5	41.11	39.1
[PVdF(HFP)-EMIM (Br)] (4:6)	T <sub>c1</sub> = 79.9, T <sub>c2</sub> = 122.8	T <sub>m1</sub> = 104.9, T <sub>m2</sub> = 132.3	8.88	8.45
[PVdF(HFP)-EMIM (Br)] (3:7)	118	128.9	-	-
[(PVdF(HFP)-EMIM (Br)] (3:7)] (30wt %)- {PC-Mg(ClO <sub>4</sub> ) <sub>2</sub> (0.3 M)] (70wt%)	80.04, 127.67	108, 133.3	-	-

and is found to be 0.02 eV. The parameters of optimized system are well-suited for supercapacitor application.

#### Research data for this article

Data will be made available on request.

#### CRediT authorship contribution statement

**Ashish Gupta:** Investigation, Validation, Software, Formal analysis, Data curation, Visualization. **Amrita Jain:** Conceptualization, Data curation, Writing - original draft, Visualization. **S.K. Tripathi:** Conceptualization, Supervision, Formal analysis, Visualization, Writing - review & editing, Funding acquisition.

#### Declaration of Competing Interest

The authors declare that they have no known competing financial interests or personal relationships that could have appeared to influence the work reported in this paper.

#### Acknowledgements

The authors are grateful to the Madhya Pradesh Council of Science and Technology, Madhya Pradesh, India for providing financial support to Prof. S.K.Tripathi through Grant-in-Aid for Scientific Research vide sanction no. [3683/CST/R&D/Phy & Engg. Sc/2012; Bhopal, Dated: 03.11.2012]. Authors are also thankful to Jaypee University of Engineering and Technology, Guna, India for providing electrochemical and electrical characterization facilities. We are also thankful to Dr. J.K.

Bera, Department of Chemistry, IIT Kanpur for providing FTIR facilities, Dr. Kamlesh Pandey, NCEMP, Allahabad for providing SEM facilities, Dr. Ajay Gupta and Dr. Mukul Gupta, UGC-DAE Consortium for Scientific Research, Indore-centre for providing the XRD facility and STIC, Cochin University, Kerala, for DSC measurement.

## Supplementary materials

Supplementary material associated with this article can be found, in the online version, at [doi:10.1016/j.est.2020.101723](https://doi.org/10.1016/j.est.2020.101723).

## References

- [1] Q. Zhao, S. Stalin, C.-Z. Zhao, L.A. Archer, Designing solid-state electrolytes for safe, energy-dense batteries, *Nat. Rev. Mater.* 5 (2020) 229–252, <https://doi.org/10.1038/s41578-019-0165-5>.
- [2] C. Zhong, Y. Deng, W. Hu, J. Qiao, L. Zheng, J. Zhang, A review of electrolyte materials and compositions for electrochemical supercapacitors, *Chem. Soc. Rev.* 44 (2015) 7484–7539, <https://doi.org/10.1039/C5CS00303B>.
- [3] E. Quartarone, P. Mustarelli, Electrolytes for solid-state lithium rechargeable batteries: recent advances and perspectives, *Chem. Soc. Rev.* 40 (2011) 2525–2540, <https://doi.org/10.1039/C0CS00081G>.
- [4] Y.S. Ye, J. Rick, B. Joe Hwang, Ionic liquid polymer electrolytes, *J. Mater. Chem. A* 1 (2013) 2719–2743, <https://doi.org/10.1039/C2TA00126H>.
- [5] M.Y. Ghotbi, Solid state electrolytes for electrochemical energy devices, *J. Mater. Sci. Mater. Electron* 30 (2019) 13835–13854, <https://doi.org/10.1007/s10854-019-01749-4>.
- [6] R.C. Agrawal, G.P. Pandey, Solid polymer electrolytes: materials designing and all-solid-state battery applications: an overview, *J. Phys. D: Appl. Phys.* 41 (2008) 223001, <https://doi.org/10.1088/0022-3727/41/22/223001>.
- [7] K.S. Ngai, S. Ramesh, K. Ramesh, J.C. Juan, A review of polymer electrolytes: fundamental, approaches and applications, *Ionics* 22 (2016) 1259–1279, <https://doi.org/10.1007/s11581-016-1756-4>.
- [8] R. Scrosati, *Applications of Electroactive Polymers*, Chapman Hall, London, 1993.
- [9] F.M. Gray, *Solid Polymer Electrolytes: Fundamentals and Technological Applications*, VCH Publishers, New York, 1991.
- [10] G.P. Pandey, S.A. Hashmi, Ionic liquid 1-ethyl-3-methylimidazolium tetracyanoborate-based gel polymer electrolyte for electrochemical capacitors, *J. Mater. Chem. A* 1 (2013) 3372–3378, <https://doi.org/10.1039/C2TA01347A>.
- [11] J.Y. Song, Y.Y. Wang, C.C. Wan, Review of gel-type polymer electrolytes for lithium-ion batteries, *J. Power Sourc.* 77 (1999) 183–197, [https://doi.org/10.1016/S0378-7753\(98\)00193-1](https://doi.org/10.1016/S0378-7753(98)00193-1).
- [12] Z. Dong, Q. Zhang, C. Yu, J. Peng, J. Ma, X. Ju, M. Zhai, Effect of ionic liquid on the properties of poly(vinylidene fluoride)-based gel polymer electrolytes, *Ionics* 19 (2013) 1587–1593, <https://doi.org/10.1007/s11581-013-0905-2>.
- [13] D. Kumar, S.A. Hashmi, Ionic liquid based sodium ion conducting gel polymer electrolytes, *Solid State Ionics* 181 (2010) 416–423, <https://doi.org/10.1016/j.ssi.2010.01.025>.
- [14] S. Ramesh, O.P. Ling, Effect of ethylene carbonate on the ionic conduction in poly(vinylidene fluoride-hexafluoropropylene) based solid polymer electrolytes, *Polym. Chem.* 1 (2010) 702–707, <https://doi.org/10.1039/B9PY00244H>.
- [15] K.S. Kim, S.Y. Park, S. Choi, H. Lee, Ionic liquid-polymer gel electrolytes based on morpholinium salt and PVdF(HFP) copolymer, *J. Power Sourc.* 155 (2006) 385–390, <https://doi.org/10.1016/j.jpowsour.2005.05.018>.
- [16] S.H. Yeon, K.S. Kim, S. Choi, J.H. Cha, H. Lee, Characterization of PVdF(HFP) gel electrolytes based on 1-(2-Hydroxyethyl)-3-methyl imidazolium ionic liquids, *J. Phys. Chem. B* 109 (2005) 17928–17935, <https://doi.org/10.1021/jp052484x>.
- [17] C. Arbizzani, G. Gabrielli, M. Mastragostino, Thermal stability and flammability of electrolytes for lithium-ion batteries, *J. Power Sourc.* 196 (2011) 4801–4805, <https://doi.org/10.1016/j.jpowsour.2011.01.068>.
- [18] J.C. Jansen, K. Friess, G. Clarizia, J. Schauer, P. Izak, High ionic liquid content polymeric gel membranes: preparation and performance, *Macromolecules* 44 (2011) 39–45, <https://doi.org/10.1021/ma102438k>.
- [19] X. Zai-Lai, A. Jeličić, Fei-Peng Wang, Pierre Rabu, Alwin Friedrich, Sabine Beuermann, A. Taubert, Transparent, flexible, and paramagnetic ionogels based on PMMA and the iron-based ionic liquid 1-butyl-3-methylimidazolium tetrachloroferrate(iii) [Bmim][FeCl<sub>4</sub>], *J. Mater. Chem.* 20 (2010) 9543–9549, <https://doi.org/10.1039/C0JM01733G>.
- [20] Shalu, V.K. Singh, R.K. Singh, Development of ion conducting polymer gel electrolyte membranes based on polymer PVdF-HFP, BMIMTFSI ionic liquid and the Li-salt with improved electrical, thermal and structural properties, *J. Mater. Chem. C* 3 (2015) 7305–7308, <https://doi.org/10.1039/C5TC00940E>.
- [21] Shalu, S.K. Chaurasia, R.K. Singh, S. Chandra, Thermal stability, complexing behavior, and ionic transport of polymeric gel membranes based on polymer PVdF-HFP and Ionic Liquid, [BMIM][BF<sub>4</sub>], *J. Phys. Chem. B* 117 (2013) 897–906, <https://doi.org/10.1021/jp307694q>.
- [22] J. Reiter, O. Krejza, M. Sedlarikova, Electrochromic devices employing methacrylate-based polymer electrolytes, *Sol. Energy Mater. Sol. Cells* 93 (2009) 249–255, <https://doi.org/10.1016/j.solmat.2008.10.010>.
- [23] F. Tuerxun, Y. Abulizi, Y. NuLi, S.J. Su, J. Yang, J.L. Wang, High concentration magnesium borohydride/tetraglyme electrolyte for rechargeable magnesium batteries, *J. Power Sourc.* 276 (2015) 255–261, <https://doi.org/10.1016/j.jpowsour.2014.11.113>.
- [24] J. Wang, S. Song, R. Muchakayala, X. Hu, R. Liu, Structural, electrical, and electrochemical properties of PVA-based biodegradable gel polymer electrolyte membranes for Mg-ion battery applications, *Ionics* 23 (2017) 1759–1769, <https://doi.org/10.1007/s11581-017-1988-y>.
- [25] A.M. Grillone, S. Panero, B.A. Retamal, B. Scrosati, Proton polymeric gel electrolyte membranes based on polymethylmethacrylate, *J. Electrochem. Soc.* 146 (1999) 27–31, <https://doi.org/10.1149/1.1391559>.
- [26] S. Chandra, S.S. Sekhon, N. Arora, PMMA based protonic polymer gel electrolytes, *Ionics* 6 (2000) 112–118, <https://doi.org/10.1007/BF02375554>.
- [27] K. Mishra, T. Arif, R. Kumar, D. Kumar, Effect of Al<sub>2</sub>O<sub>3</sub> nanoparticles on ionic conductivity of PVdF-HFP/PMMA blend-based Na<sup>+</sup> ion conducting nanocomposite gel polymer electrolyte, *J. Solid State Electrochem.* 23 (2019) 2401–2409, <https://doi.org/10.1007/s10008-019-04348-9>.
- [28] Z. Li, G. Su, X. Wang, D. Gao, Micro-porous P(VDF-HFP)-based polymer electrolyte filled with Al<sub>2</sub>O<sub>3</sub> nanoparticles, *Solid State Ion* 176 (2005) 1903–1908, <https://doi.org/10.1016/j.ssi.2005.05.006>.
- [29] M. Deka, A. Kumar, Ionic transport in P(VdF-HFP)-PEO based novel microporous polymer electrolytes, *Bull. Mater. Sci.* 32 (2009) 627–632, <https://doi.org/10.1007/s12034-009-0097-6>.
- [30] D. Saikia, Y.W. Chen-Yang, Y.T. Chen, Y.K. Li, S.I. Lin, <sup>7</sup>Li NMR spectroscopy and ion conduction mechanism of composite gel polymer electrolyte: a comparative study with variation of salt and plasticizer with filler, *Electrochim. Acta* 54 (2009) 1218–1227, <https://doi.org/10.1016/j.electacta.2008.09.001>.
- [31] F.S. Freitas, N.F. Jilian, I.B. Ito, M. Paoli, A. Nogueira, Electrochemical and structural characterization of polymer gel electrolytes based on a PEO copolymer and an imidazolium-based ionic liquid for dye-sensitized solar cells, *ACS Appl. Mater. Interfaces* 1 (2009) 2870–2877, <https://doi.org/10.1021/am900596x>.
- [32] Z. Tang, L. Qi, G. Gao, Structural, thermal, and impedance properties of a gel polymer electrolyte containing ionic liquid, *Polym. Adv. Technol.* 21 (2009) 153–157, <https://doi.org/10.1002/pat.1408>.
- [33] L. Reinert, K. Batouche, J.M. Leveque, F. Muller, J.M. Beny, B. Kebabi, L. Duclaux, Adsorption of imidazolium and pyridinium ionic liquids onto montmorillonite: Characterization and thermodynamic calculations, *Chem. Eng.* 209 (2012) 13–19, <https://doi.org/10.1016/j.ccej.2012.07.128>.
- [34] M. Deepa, S.A. Agnihotry, D. Gupta, R. Chandra, Ion-pairing effects and ion-solvent-polymer interactions in LiN(CF<sub>3</sub>SO<sub>2</sub>)<sub>2</sub>-PC-PMMA electrolytes: a FTIR study, *Electrochim. Acta* 49 (2004) 373–383, <https://doi.org/10.1016/j.electacta.2003.08.020>.
- [35] G.P. Pandey, R.C. Agrawal, S.A. Hashmi, Magnesium ion conducting gel polymer electrolytes dispersed with fumed silica for rechargeable magnesium battery application, *J. Solid State Electrochem.* 15 (2011) 2253–2264, <https://doi.org/10.1007/s10008-010-1240-4>.
- [36] A. Jain, S.K. Tripathi, Nano-porous activated carbon from sugarcane waste for supercapacitor application, *J. Energy Storage* 4 (2015) 121–127, <https://doi.org/10.1016/j.est.2015.09.010>.